Magnetic properties of the Blume-Emery-Griffiths model in the vicinity of an antiferromagnetic Potts line

T. Balcerzak and M. Gzik-Szumiata
Department of Solid State Physics, University of Łódź, ul. Pomorska 149/153, PL 90-236 Łódź, Poland
(Received 11 January 1999)

The Blume-Emery-Griffiths model is studied for the range of parameters in a close neighborhood of the antiferromagnetic three-state Potts model. The cluster variational method in pair approximation is adopted for the studies. Particular attention is paid to the properties of ferrimagnetic and staggered quadrupolar phases which occur on a bipartite lattice. In particular, the isothermal susceptibility is calculated, revealing its splitting into two branches, each with different temperature behavior. The reentrant ferrimagnetism phenomenon is also discussed. [S0163-1829(99)04030-8]

I. INTRODUCTION

The Blume-Emery-Griffiths (BEG) model[1] has been intensively studied because of the very rich phase diagrams it exhibits. The model Hamiltonian contains, in addition to the bilinear interaction, both biquadratic exchange and single-ion anisotropy terms. When these terms are competing with the bilinear exchange interaction one can predict the existence of multicritical points, the occurrence of staggered quadrupolar and ferrimagnetic phases, as well as the reentrant magnetism phenomenon.

The model has been extensively studied by means of the mean-field approximation (MFA),[1–5] by renormalization-group techniques,[6,7] effective-field theory,[8–10] cluster variational method (CVM),[11–14] and by Monte Carlo simulation.[2,15,16] Some exact solutions on Bethe lattice have also been obtained.[17,18,20] Recently, the phase diagrams in a bilayer system were studied, using the cluster variational method in a pair approximation (CVMPA).[19,20]

The interesting property of the BEG model is that for certain values of parameters, describing the biquadratic exchange and single-ion anisotropy, it can be reduced to the three-state antiferromagnetic (AF) Potts model.[3,6,12,14] For the parameters in the vicinity of the AF Potts line, among several phases existing on the phase diagrams, a ferrimagnetic phase can be detected.

The ferrimagnetic phase is of particular interest since it occurs in a very narrow range of Hamiltonian parameters.[12,14,20] It emerges from either the staggered quadrupolar or ferromagnetic phases, being sandwiched between these two, as an energetically most favorable solution. To obtain this phase, it is necessary to consider the so-called bipartite lattice, i.e., the lattice which can be subdivided into two interpenetrating sublattices a and b.[18] For the AF Potts line the four phases: ferromagnetic, paramagnetic, staggered quadrupolar, and ferrimagnetic merge in the point of their coexistence (i.e., multicritical point).

The aim of the present paper is the investigation of the magnetic properties of BEG model in the vinicity of the AF Potts line, where the phase diagrams become particularly complex. For the studies we choose the CVMPA technique, as it is a relatively simple method and much more accurate than MFA.[19] Moreover, as pointed out in Ref. 20, for a Bethe lattice the results of CVMPA are exact.

In numerical calculations we studied the phase diagrams, the magnetization, quadrupolar moment, and isothermal susceptibility. Particular attention is paid to the susceptibility of the ferrimagnetic phase, which up to now has not been studied in literature. The most important results are illustrated in the figures and discussed in detail.

II. THEORY

The Hamiltonian of the system is of the form:

$$H=-J\sum_{\langle ij\rangle} S_iS_j-A\sum_{\langle ij\rangle} S_i^2S_j^2-D\sum_i S_i^2-h\sum_i S_i, \quad (1)$$

where $S_i=0,\pm 1$. The constant parameters J and A are, respectively, the nearest-neighbor (NN) bilinear and biquadratic exchange interactions, whereas D denotes single-ion anisotropy and h stands for an external field.

In CVMPA, the Gibbs free energy per 1 spin can be obtained from the formula[20]

$$\frac{G}{N}=\frac{1}{2\beta}[(z-1)(\ln Z_a+\ln Z_b)-z\ln Z_{ab}], \quad (2)$$

where $\beta=1/k_BT$, and z is the number of nearest neighbors. In Eq. (2), Z_a and Z_b are the partition functions for one-atom clusters corresponding to the a or b sublattice, respectively, whereas Z_{ab} is the two-atom cluster partition function. These functions are given in the form

$$Z_\alpha=u(e^{\beta h}p_\alpha+e^{-\beta h}l_\alpha)+1 \quad (\alpha=a,b) \quad (3)$$

and

$$Z_{ab}=u^2f(e^{2\beta h}p_a^np_b^n+e^{-2\beta h}l_a^nl_b^n)+u^2g(p_a^nl_b^n+p_b^nl_a^n)+ue^{\beta h}(p_a^n+p_b^n)+ue^{-\beta h}(l_a^n+l_b^n)+1, \quad (4)$$

where

$$u=e^{\beta D}, \quad (5)$$

$$f=e^{\beta A}e^{\beta J}, \quad (6)$$

and

$$g = e^{\beta A} e^{-\beta J}. \tag{7}$$

The quantities p_α and l_α are defined by the formulas

$$p_\alpha = \exp[\beta(AK_\alpha + J\Lambda_\alpha)], \tag{8}$$

$$l_\alpha = \exp[\beta(AK_\alpha - J\Lambda_\alpha)], \tag{9}$$

where Λ_α and K_α $(\alpha = a,b)$ are the variational parameters and they represent the dipolar and quadrupolar effective fields, respectively. For the equilibrium, in the presence of the external field, these parameters can be found from the cluster variational equations:

$$p_a = p_a^n \frac{1+u(fe^{\beta h}p_b^n + ge^{-\beta h}l_b^n)}{1+u(e^{\beta h}p_b^n + e^{-\beta h}l_b^n)},$$

$$p_b = p_b^n \frac{1+u(fe^{\beta h}p_a^n + ge^{-\beta h}l_a^n)}{1+u(e^{\beta h}p_a^n + e^{-\beta h}l_a^n)},$$

$$l_a = l_a^n \frac{1+u(fe^{-\beta h}l_b^n + ge^{\beta h}p_b^n)}{1+u(e^{-\beta h}l_b^n + e^{\beta h}p_b^n)},$$

$$l_b = l_b^n \frac{1+u(fe^{-\beta h}l_a^n + ge^{\beta h}p_a^n)}{1+u(e^{-\beta h}l_a^n + e^{\beta h}p_a^n)}, \tag{10}$$

where $n=(z-1)/z$. One can see that for $h \to 0$ the above equations reduce to the form given in Ref. 20. With the help of p_α and l_α, the sublattice magnetizations $m_\alpha \equiv \langle S_i \rangle_\alpha$ and quadrupolar moments $q_\alpha \equiv \langle S_i^2 \rangle_\alpha$ $(q_\alpha \geqslant 0)$ can be found. For the equilibrium they are given by the formulas

$$m_\alpha = \frac{u}{Z_\alpha}(e^{\beta h}p_\alpha - e^{-\beta h}l_\alpha) \tag{11}$$

and

$$q_\alpha = \frac{u}{Z_\alpha}(e^{\beta h}p_\alpha + e^{-\beta h}l_\alpha). \tag{12}$$

The various phases of the two sublattice model with $J>0$ are then defined as follows:

ferromagnetic phase (F): $m_a = m_b \neq 0,\ q_a = q_b$;

paramagnetic phase (P): $m_a = m_b = 0,\ q_a = q_b$;

staggered quadrupolar phase (SQ): $m_a = m_b = 0,\ q_a \neq q_b$;

ferrimagnetic phase (I): $0 \neq m_a \neq m_b \neq 0,\ q_a \neq q_b$.

Thus, the various phases can be identified by examing the solutions for m_α and q_α, resulting from Eqs. (11) and (12).

On the other hand, the total equilibrium magnetization of the system can be found from the thermodynamic relationship:

$$M \equiv -\left(\frac{\partial G}{\partial h}\right)_T = \frac{N}{2}(m_a + m_b). \tag{13}$$

The derivative in Eq. (13) is taken for a constant temperature. The second derivative over the external field gives the isothermal susceptibility of the system:

$$\chi_T \equiv -\left(\frac{\partial^2 G}{\partial h^2}\right)_T = \left(\frac{\partial M}{\partial h}\right)_T = \frac{N}{2}\left[\left(\frac{\partial m_a}{\partial h}\right)_T + \left(\frac{\partial m_b}{\partial h}\right)_T\right]. \tag{14}$$

Hence, the susceptibility per one lattice site can be written in the form

$$\frac{J}{N}\chi_T = \frac{1}{2}(\chi_a + \chi_b), \tag{15}$$

where, taking into account Eqs. (11) and (12), the sublattice susceptibility χ_α $(\alpha = a,b)$ is expressed as

$$\chi_\alpha = J\beta[v_\alpha C_\alpha + u_\alpha(B_\alpha + 1)]. \tag{16}$$

In Eq. (16) we have introduced the abbreviated notation:

$$v_\alpha = m_\alpha(1 - q_\alpha), \tag{17}$$

$$u_\alpha = q_\alpha - m_\alpha^2, \tag{18}$$

and

$$B_\alpha = J\left(\frac{\partial \Lambda_\alpha}{\partial h}\right)_T, \tag{19}$$

$$C_\alpha = A\left(\frac{\partial K_\alpha}{\partial h}\right)_T. \tag{20}$$

In turn, the coefficients B_α and C_α can be obtained by differentiation of the cluster variational equations (10). After some algebra, one obtains the set of linear equations in the form

$$\begin{aligned}
&u_a B_a - (z-1)t_{11}B_b + v_a C_a - (z-1)t_{12}C_b = zt_{11}\\
&-(z-1)t_{11}B_a + u_b B_b - (z-1)t_{21}C_a + v_b C_b = zt_{11},\\
&v_a B_a - (z-1)t_{21}B_b + w_a C_a - (z-1)t_{22}C_b = zt_{21}\\
&-(z-1)t_{12}B_a + v_b B_b - (z-1)t_{22}C_a + w_b C_b = zt_{12},
\end{aligned} \tag{21}$$

where v_α and u_α are given by Eqs. (17) and (18), respectively, and

$$w_\alpha = q_\alpha(1 - q_\alpha) \quad (\alpha = a,b). \tag{22}$$

Other coefficients in Eq. (21), namely t_{xy} are the NN correlation functions defined as

$$\begin{aligned}
t_{11} &= \langle S_a S_b \rangle - m_a m_b,\\
t_{12} &= \langle S_a S_b^2 \rangle - m_a q_b,\\
t_{21} &= \langle S_a^2 S_b \rangle - q_a m_b,\\
t_{22} &= \langle S_a^2 S_b^2 \rangle - q_a q_b.
\end{aligned} \tag{23}$$

Consequently, these spin-spin correlations can be obtained within CVMPA. For instance, in the limit $h \to 0$ their final forms can be written as

$$\langle S_a S_b \rangle = \frac{1}{Z_{ab}} [u^2 f(p_a^n p_b^n + l_a^n l_b^n) - u^2 g(p_a^n l_b^n + p_b^n l_a^n)],$$

$$\langle S_a S_b^2 \rangle = \frac{1}{Z_{ab}} [u^2 f(p_a^n p_b^n - l_a^n l_b^n) + u^2 g(p_a^n l_b^n - p_b^n l_a^n)],$$

$$\langle S_a^2 S_b \rangle = \frac{1}{Z_{ab}} [u^2 f(p_a^n p_b^n - l_a^n l_b^n) - u^2 g(p_a^n l_b^n - p_b^n l_a^n)],$$

$$\langle S_a^2 S_b^2 \rangle = \frac{1}{Z_{ab}} [u^2 f(p_a^n p_b^n + l_a^n l_b^n) + u^2 g(p_a^n l_b^n + p_b^n l_a^n)]. \tag{24}$$

The practical procedure based on the above theoretical method can be outlined as follows:

(1) First we need to solve the cluster variational equations (10) representing the necessary equilibrium conditions. Having p_α and l_α, the magnetizations m_α and quadrupolar moments q_α can be calculated from Eqs. (11) and (12).

(2) Among various possible solutions of m_α and q_α we choose that one which corresponds to the lowest Gibbs energy (2). This criterion ensures that we are considering the stable phase only (see the phase diagrams obtained in Ref. 20).

(3) Having stable solutions for p_α and l_α, as well as m_α and q_α, we can calculate the coefficients $v_\alpha, u_\alpha, w_\alpha$ [Eqs. (17), (18), and (22)] and the correlation functions t_{xy} [Eq. (23)]. Hence, all coefficients appearing in the set of linear equations (21) are known. These coefficients depend only on the temperature and the Hamiltonian parameters J, A, and $D(h \to 0)$.

(4) The linear set of equations (21) can be solved with respect to the B_α and C_α variables.

(5) Finally, with the help of B_α and C_α, the sublattice isothermal susceptibilities χ_α can be calculated from Eq. (16).

The numerical results based on the method outlined above will be presented in the next section.

III. THE NUMERICAL RESULTS AND DISCUSSION

On the basis of the theory presented in previous section the numerical calculations have been made. We chose the most interesting case when the phase diagrams exhibit the presence of ferrimagnetic phase, and its coexistence with other phases in the vicinity of the AF Potts point ($A/J = -3$; $D/J = 2z$, $h = 0$).[3,6,12,14] For comparison, the calculations have been made for $z = 4$ (monoatomic layer) and $z = 5$, corresponding to a double-layer system with simple cubic symmetry.

In Fig. 1 the phase diagram $k_B T/J$ vs A/J for $D/J = 8$ and $z = 4$ is presented. As it has been stated, for the particular value $A/J = -3$, the BEG model reduces then to the three-state AF Potts model. The regions of coexistence of ferromagnetic (F), paramagnetic (P), staggered quadrupolar (SQ), and ferrimagnetic (I) phases are indicated. All these phases meet at the multicritical point which is denoted by the bold dot. It is worth noticing that the I phase is separated from the SQ phase by the second-order transition line and it exists in a very narrow range of the A/J parameter.[18] The I and F phases are separated by the first-order transitions (AF Potts line, dashed).

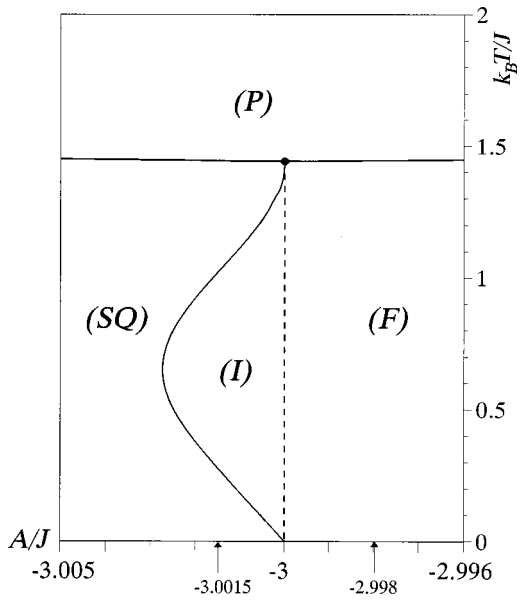

FIG. 1. The phase diagram $k_B T/J$ vs A/J for $z = 4$ and $D/J = 8$. The AF Potts line (dashed) represents the first-order transitions. The multicritical point is marked by a dot.

In Fig. 2 we present the magnetization vs temperature for ferromagnetic phase at $A/J = -2.998$. We see that the magnetization quite unexpectedly changes rapidly for very low temperatures, whereas for higher temperatures its behavior is typical.

In Fig. 3 the isothermal susceptibility is presented for the same parameters as in Fig. 2. Apart from a typical singularity at the Curie temperature, a remarkable increase of susceptibility for very low temperatures is observed. This increase is related to the anomalous behavior of magnetization, as shown in Fig. 2.

In Fig. 4 we present the magnetization vs temperature for

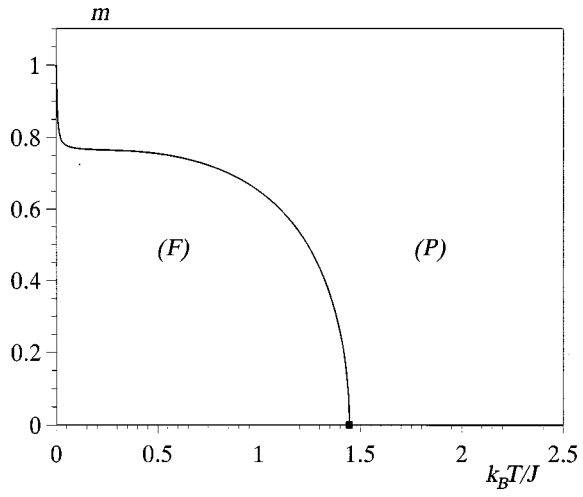

FIG. 2. Magnetization m per one lattice site vs temperature $k_B T/J$ for $z = 4$, $D/J = 8$, and $A/J = -2.998$.

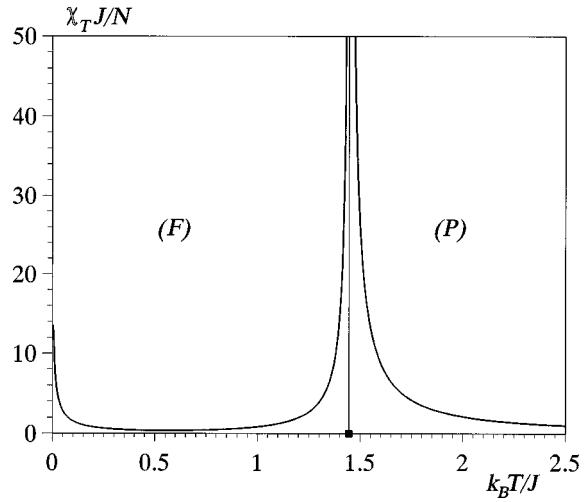

FIG. 3. The dimensionless susceptibility per one lattice site, $\chi_T J/N$ vs temperature k_BT/J for the same parameters as in Fig. 2.

$A/J=-3.0015$, the value which is chosen from the opposite side of the Potts line. In this case, due to the existence of the I phase, the reentrant phenomenon is seen. Two branches of magnetization, each corresponding to its sublattice are shown. On the other hand, in the SQ phase the magnetizations of both sublattices are equal to zero, whereas the quadrupolar moments $q_a \neq q_b \geqslant 0$. This splitting of the quadrupolar moments is also observed in the ferrimagnetic phase, however we do not present it in the figure.

It is interesting to see the behavior of isothermal susceptibility vs temperature for the same parameters as in Fig. 4. The results of the calculations are presented in Fig. 5. Two branches of the susceptibility in the I and SQ phases, corresponding to *a* and *b* sublattices, are seen. The mean value of the susceptibility is indicated by the dashed line. In two phase-transition points between the SQ and I phase these susceptibilities diverge. For $T \to 0$ the sublattice susceptibilities reveal quite different behavior: one of them diverges, whereas the other one tends to zero. At the phase-transition

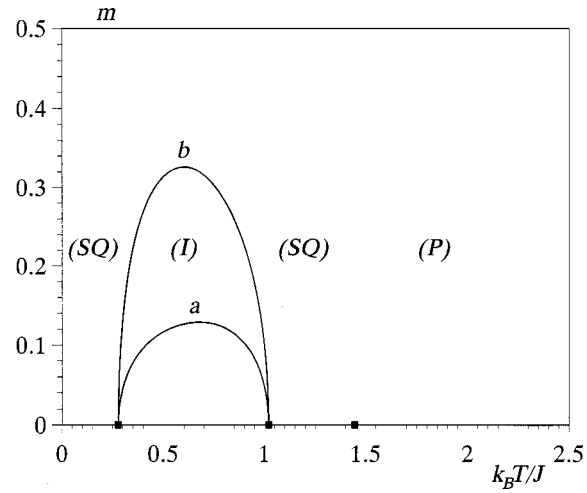

FIG. 4. The sublattice magnetizations (*a* and *b* curves) per one lattice site vs temperature k_BT/J for $z=4$, $D/J=8$, and $A/J=-3.0015$. The reentrant ferrimagnetism is accompanied by the second-order phase transition.

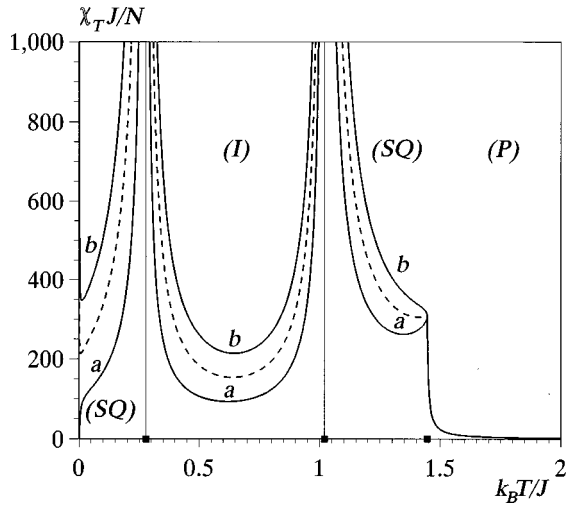

FIG. 5. The sublattice susceptibilities (*a* and *b* curves) per one lattice site vs temperature k_BT/J for the same parameters as in Fig. 4. The curves *a* and *b* correspond to *a* and *b* lines from Fig. 4, respectively. The dashed line represents the mean value of the susceptibility.

point between the SQ and P phase both curves merge to their common finite value.

Change of the coordination number from $z=4$ to $z=5$ has a great influence on the phase diagram. For $z=5$ and $D/J=10$ the phase diagram k_BT/J vs A/J is presented in Fig. 6 around the Potts line ($A/J=-3$). In this case two ferrimagnetic phases instead of one, namely, the low- and high-temperature phases are seen. The first-order transitions are indicated by the dashed line, whereas the continuous lines represents the second-order (continuous) transitions. Such phase diagrams have already been documented in the literature.[12,14,20] In the following figures we chose the values $A/J=-2.998$ and $A/J=-3.0005$ in order to present the magnetic properties vs dimensionless temperature.

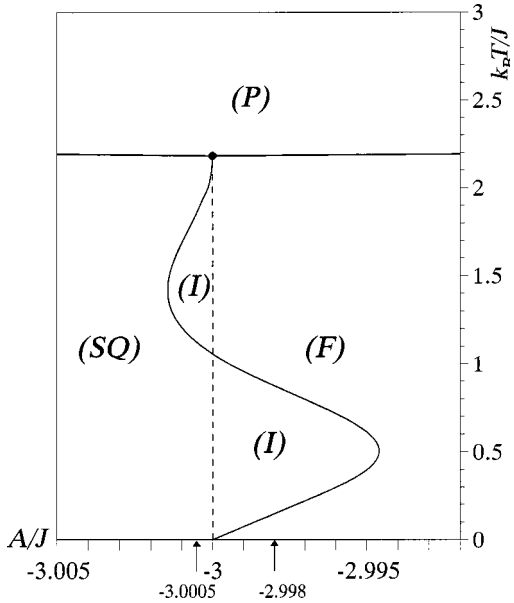

FIG. 6. The phase diagram k_BT/J vs A/J for $z=5$ and $D/J=10$. The AF Potts line (dashed) represents the first-order transitions. The multicritical point is marked by a dot.

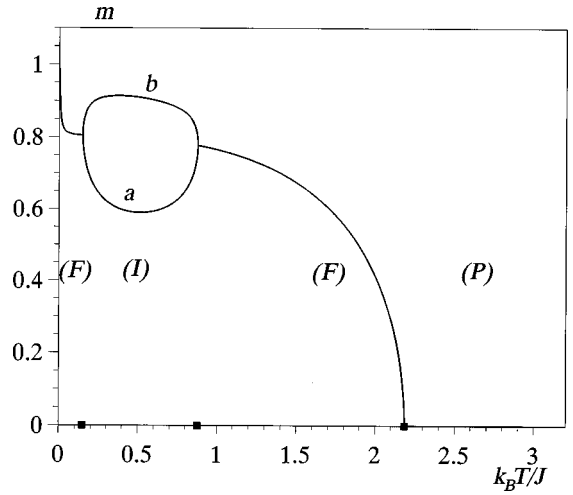

FIG. 7. Magnetization m per one lattice site vs temperature k_BT/J for $z=5$, $D/J=10$, and $A/J=-2.998$. The curves a and b correspond to the sublattice magnetizations in the ferrimagnetic phase.

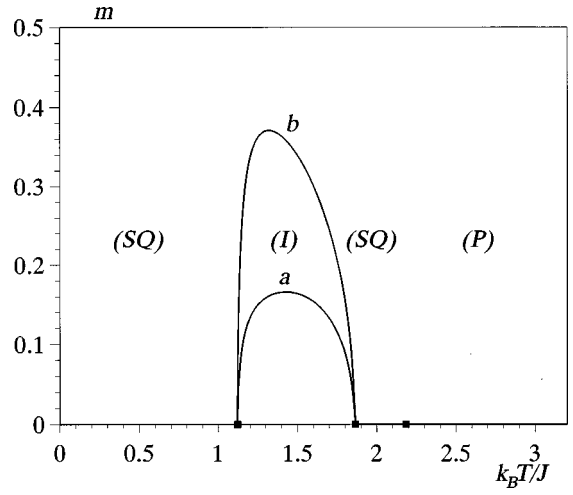

FIG. 9. The sublattice magnetizations (a and b curves) per one lattice site vs temperature k_BT/J for $z=5$, $D/J=10$, and $A/J=-3.0005$. The reentrant ferrimagnetism is terminated by the second-order phase transitions.

In Fig. 7 the magnetization vs temperature for $A/J=-2.998$ is shown. The splitting of the magnetization into two branches in the ferrimagnetic phase is very evident. For low temperatures the magnetization curve changes rapidly tending to 1, which is similar to that observed in Fig. 2.

The magnetic susceptibility vs temperature for the same parameters as in Fig. 7 is presented in Fig. 8. In this case three phase-transition points exist, namely F/I, I/F, and F/P phase transitions. The susceptibility in the I phase is of particular interest: one of the sublattice susceptibilities (that corresponding to higher magnetization) becomes negative. Both curves diverge at the phase-transition points when these points are approached from the I phase, whereas outside the I region the susceptibility tends to a finite value. The negative value of one sublattice susceptibility can be explained on the basis of the magnetization curve from Fig. 7. As we have seen, the splitting of sublattice magnetization there was quite strong. In a small external field the system becomes more ordered, that is, the magnetization of the a sublattice slightly increases whereas the magnetization of the b sublattice diminishes, both curves tending to some intermediate value. It is worth noticing that the mean value of those sublattice susceptibilities is positive, as it is presented by the dashed line in Fig. 8. The remaining parts of the susceptibility curves, i.e., those in the F and P phases, are similar to the analogous behavior from Fig. 3. In particular, for $T\rightarrow 0$ the susceptibility increases, which is again connected with the anomalous behavior of the magnetization.

In Fig. 9 we present the magnetization vs temperature for $A/J=-3.0005$. The reentrant magnetism phenomenon for the I phase is seen. Both sublattice magnetizations exhibit continuous SQ/I phase transitions and the picture is qualitatively similar to that of Fig. 4.

For completeness, Fig. 10 presents the susceptibility vs

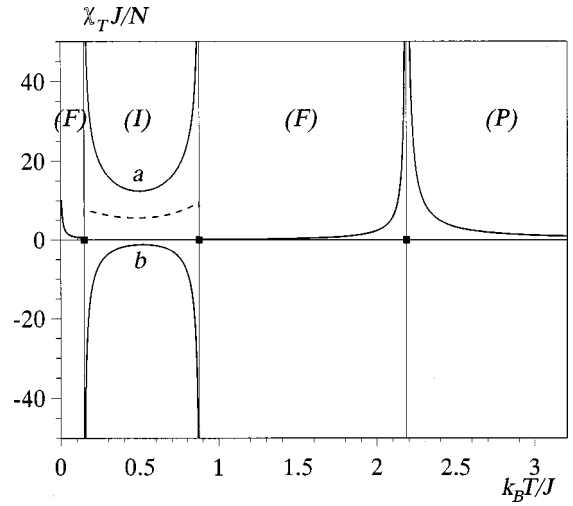

FIG. 8. The dimensionless magnetic susceptibility per one lattice site $\chi_T J/N$ vs temperature k_BT/J for the same parameters as in Fig. 7. The curves a and b denote the sublattice susceptibilities and correspond to curves a and b from Fig. 7, respectively. By the dashed line the mean value of the susceptibility is shown.

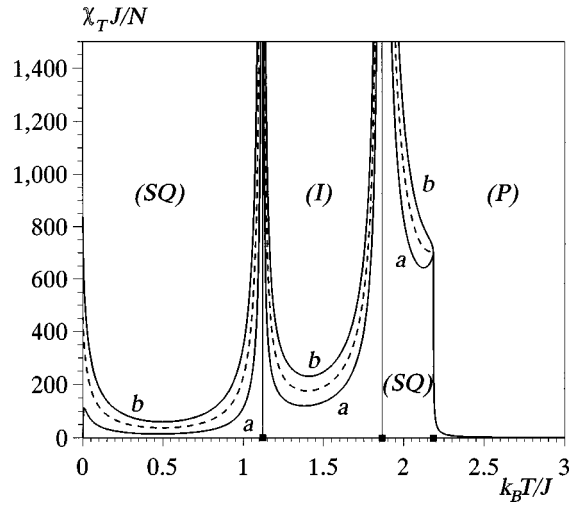

FIG. 10. The sublattice susceptibility (a and b curves) per one lattice site vs temperature k_BT/J for the same parameters as in Fig. 9. The curves a and b correspond to a and b from Fig. 9, respectively. The dashed line represents the mean value of the susceptibility.

temperature for the same parameters as in Fig. 9. In this case the picture is qualitatively similar to that presented in Fig. 5. The continuous phase transitions between the SQ and I phases, as seen in the phase diagram (Fig. 6), are again confirmed by the singularities of the sublattice susceptibilities. The mean value of the susceptibility in the SQ and I phases is indicated by the dashed lines. Let us note that the susceptibility in the P phase is relatively small and rapidly diminishes with the increase of the temperature.

IV. FINAL REMARKS

In the paper we studied the magnetic properties of the BEG model in a vinicity of the AF Potts line. The comparison of $z=4$ (planar system) with $z=5$ (bilayer) has been made. In particular, the phase diagrams occurred differently for these two cases, since for $z=5$ two ferrimagnetic regions are predicted, instead of one I region existing for $z=4$.

The topology of these two diagrams has been confirmed by the magnetization and quadrupolar moment calculations. However, only the magnetization (being a measurable quantity) has been presented in the figures.

In the frame of the uniform method, based on the Gibbs energy calculations, the static isothermal susceptibility has been obtained. As far as we know, the calculations of susceptibility for the ferrimagnetic phase are primary within CVMPA. The following interesting phenomena should be pointed out: First, two branches of the susceptibility have been obtained in the I and SQ phases. With regard to the SQ phase, similar splitting has been reported in the frame of MFA,[5] although the phase diagrams there were quite different. The calculations performed here for the low-temperature SQ phase show also completely different behavior for these two sublattice susceptibilities, which has not yet been reported. Second, the negative branch of one sublattice susceptibility for $z=5$ (Fig. 8) is worth noticing. As we pointed out, this phenomenon occurs only from one side of the Potts line, where the I phase is surrounded by the F phase. From the other side, where the I phase is surrounded by the SQ phase both sublattice susceptibilities are positive. Hence, we would like to conclude that the influence of the surrounding phase on the ferrimagnetic region can be crucial. This fact can be explained from the energetic point of view, since these two neighboring phases are characterized by the comparable free energies.

Finally, we are convinced that CVMPA proved to be a useful technique for investigations of such detailed and subtle effects. It has been shown that the predictions of CVMPA for the BEG model are much more accurate than MFA.[19] Moreover, as pointed out in Ref. 20 the method is equivalent to the exact Bethe lattice theory. For regular lattices, however, some improvement can be introduced by means of more advanced cluster variational methods, for instance in eight-point ''cube'' approximation.[12] Therefore, it would be useful to employ MC simulations to verify some of characteristic predictions reported in the present paper. To perform such simulations the range of parameter values around the Potts line can be established on the basis of our results. It would be also interesting to obtain the magnetic contribution to the specific heat in the frame of the same method. This is planned for a future work.

[1] M. Blume, V. J. Emery, and R. B. Griffiths, Phys. Rev. A **4**, 1071 (1971).
[2] M. Tanaka and T. Kawabe, J. Phys. Soc. Jpn. **54**, 2194 (1985).
[3] W. Hoston and A. N. Berker, Phys. Rev. Lett. **67**, 1027 (1991).
[4] J. A. Plascak, J. G. Moreira, and F. C. Sá Barreto, Phys. Lett. A **173**, 360 (1993).
[5] M. Gzik and T. Balcerzak, Acta Phys. Pol. A **92**, 543 (1997).
[6] A. N. Berker and M. Wortis, Phys. Rev. B **14**, 4946 (1976).
[7] R. R. Netz and A. N. Berker, Phys. Rev. B **47**, 15 019 (1993).
[8] T. Kaneyoshi, J. Phys. Soc. Jpn. **56**, 4199 (1987).
[9] J. W. Tucker, J. Magn. Magn. Mater. **80**, 203 (1989).
[10] M. Jaščur and T. Kaneyoshi, Phys. Status Solidi B **174**, 537 (1992).
[11] A. Rosengren and S. Lapinskas, Phys. Rev. B **47**, 2643 (1993).
[12] A. Rosengren and S. Lapinskas, Phys. Rev. Lett. **71**, 165 (1993).
[13] G. Grigelionis and A. Rosengren, Physica A **208**, 287 (1994).
[14] S. Lapinskas and A. Rosengren, Phys. Rev. B **49**, 15 190 (1994).
[15] Y. L. Wang and C. Wentworth, J. Appl. Phys. **61**, 4411 (1987).
[16] D. Wingert and D. Stauffer, Physica A **219**, 135 (1995).
[17] R. Osório, M. J. Oliveira, and S. R. Salinas, J. Phys.: Condens. Matter **1**, 6687 (1989).
[18] A. Z. Akheyan and N. S. Ananikian, J. Phys. A **29**, 721 (1996).
[19] T. Balcerzak and M. Gzik (unpublished).
[20] J. W. Tucker, T. Balcerzak, M. Gzik, and A. Sukiennicki, J. Magn. Magn. Mater. **187**, 381 (1998).